ISSN 2176-5480

22nd International Congress of Mechanical Engineering (COBEM 2013)
November 3-7, 2013, Ribeirão Preto, SP, Brazil

APPLICATION OF CFD-DEM COUPLING IN THE PREDICTION OF THE FLOW DYNAMICS OF AN ALUMINA FLUIDIZED BED

Alan Mota Castelo Branco Júnior
André Luiz Amarante Mesquita
Jerson Rogério Pinheiro Vaz
Universidade Federal do Pará, Lab. de Eng. Mecânica, Rua Augusto Corrêa, 01- Belém, Pará, Brasil – CEP 66075-110
motacastelo2008@hotmail.com, andream@ufpa.br, jerson@ufpa.br

Abstract. *The coupling between CFD and DEM have become attractive for the simulation of gas-solid flows and was used in this work to predict the behavior of an alumina fluidized bed. In order to develop a model capable of confidently predicting the alumina bed's behavior for different operating conditions it were analyzed the effects of using different drag models. The representation of the particles was conducted with both uniform size and particle size distribution. Predictions of important data like the minimum fluidization velocity and the gas pressure drop through the bed were obtained. The simulations were carried out by using the software ANSYS FLUENT v.14.5, considering an Eulerian approach for the fluid phase and explicitly resolving the particle interactions by the Discrete Element Method (DEM). The results of the simulations were compared to experimental data, showing good agreement in terms of global behavior, despite the use of a linear contact model and unrealistic low values for the particle spring constant. However, it was verified that care must be taken when setting parameters like CFD and DEM time steps and choosing the drag model, in order to assure acceptable results.*

Keywords: *CFD-DEM, Fluidized bed, Multiphase Flow, Alumina, ANSYS FLUENT*

1. INTRODUCTION

The fluidization process has several applications in many kinds of industries, mainly due to some of its characteristics like temperature uniformity, excellent surface-to-bed heat transfer and the high mixing rate between the solid and the fluid phases (Crowe, 2006). According to Niemi (2012), in the simulation of dense gas-solid flows, like in fluidized beds, there are two basic approaches regarding how to model the gas-solid system: the Eulerian-Eulerian approach and the Eulerian-Lagrangian approach. Due to the fact that from a macroscopic viewpoint the solid phase in a fluidized bed behaves like a kind of fluid, many computational simulations of fluidized beds have been based on the Euler-Euler approach, which regards both the gas and the granular solid phases as two fluids, also using generalized Navier-Stokes equations for both phases (Tsuji et al., 1993).

However, in the Euler-Euler approach the modeling of constitutive relations for the governing equations is a challenging task and due to the diverse nature of different multiphase flows those relations will be largely case dependent. If good agreement between numerical simulations and experiments is required, some parameters in the constitutive equations should be determined empirically and sometimes even from experiments similar to the simulations to be done. Also, in the Euler-Euler approach the inclusion of particle size distribution (PSD) which is important to the analysis of many systems like those which involve particle segregation is not as straightforward. In general, only average particle properties are considered, since the inclusion of PSD requires the usage of additional equations or sub-models which can substantially increase the computational demands (Niemi, 2012).

The coupling between the CFD (Computational Fluid Dynamics) and the DEM (Discrete Element Method) follows the Euler-Lagrange approach (Zhu et al., 2007). With the CFD-DEM coupling the behavior of the fluid phase is analyzed by the CFD and the behavior each individual particle is analyzed by the Newtonian equations of motion, in which the forces acting on the particles due to the interactions with other particles and walls are calculated by the force-displacement laws of the DEM. A review of works in which the CFD-DEM coupling has been applied to the fluidization of cohesive and cohesionless particles including both monosized and multi-sized particle systems can be found in Zhu et al. (2008).

The main drawback of using the DEM for analyzing the behavior of particles is the high demand in terms of computing power, since large scale industrial systems usually involve a prohibitively high number of particles, what it leads to the need for strategies like, for example, the usage of virtual particles with diameters greater than the diameters of the real particles (Hilton and Cleary, 2012). According to Malone and Xu (2008) several other approaches have been used to reduce the computational load of DEM and allow larger number of particles to be simulated within a reasonable timescale. These include the use of more advanced contact detection algorithms (Iwai et al., 1999), parallel computing techniques (Fleissner and Eberhard, 2008), novel numerical time integration schemes (Fraige and Langston, 2004), and more commonly in the case of simple linear-spring-dashpot (LSD) models, selecting a small value of the particle spring constant, which permits a larger time step to be used (Tsuji et al., 1993; Limtrakul et al., 2003; Mikami et al., 1998; Rhodes et al., 2001).

ISSN 2176-5480

The aim of the present work is to investigate the applicability of the CFD-DEM coupling in the analysis of practical problems faced in some industries of the state of Pará, more specifically the fluidization of alumina used in the aluminum industry. According to Brazil's National Mining Plan 2030 (MME, 2011), the aluminum is the second most produced metal worldwide, mainly due to its characteristics and the existence of large bauxite mines. When it comes to bauxite production, Brazil has a leading position in the international market, being the second in the world ranking. The world bauxite reserves are of about 34 billion tons and, in Brazil, they are of about 3.4 billion tons, mainly in the states of Minas Gerais and Pará. About 96% of the national production of metallurgical bauxite is intended for the production of alumina (aluminum oxide), which is used in the production of aluminum.

2. MODEL DESCRIPTION

In the CFD-DEM model used for the simulation of the fluidized bed the modelling of the continuous gas phase is carried out by means of the Eulerian approach, sometimes referred to as Multi Fluid approach, in which the volume fraction of the phase is included in its governing partial differential equations. The modeling of the discrete solid phase is carried out by means of the Lagrangian approach, in which the motion of representative particles are tracked by means of ordinary differential equations related to the Newton's Law of motion and the particles collision forces are determined by the Discrete Element Method.

2.1 Gas phase

Since in the present work heat and mass transfer, as well as chemical reactions are not considered, the set of governing equations for the continuous gas phase (air) is written as (Gidaspow, 1994):

$$\frac{\partial}{\partial t}\left(\alpha_q \rho_q\right) + \nabla.\left(\alpha_q \rho_q \boldsymbol{v}_q\right) = 0 \tag{1}$$

$$\frac{\partial}{\partial t}\left(\alpha_q \rho_q \boldsymbol{v}_q\right) + \nabla.\left(\alpha_q \rho_q \boldsymbol{v}_q \boldsymbol{v}_q\right) = -\alpha_q \nabla P + \nabla.\,\bar{\bar{\tau}}_q + \alpha_q \rho_q \boldsymbol{g} + K_{pq}\left(\boldsymbol{v}_p - \boldsymbol{v}_q\right) + S_{other} \tag{2}$$

where α_q, ρ_q and $\boldsymbol{v}_q$ are, respectively, the volume fraction, density and velocity of the gas, P is the pressure, $\bar{\bar{\tau}}_q$ is the stress-strain tensor, $\boldsymbol{g}$ is the acceleration due to gravity and $\boldsymbol{v}_p$ is the velocity of the solid phase. The term K_{pq} is the interphase momentum exchange coefficient due to drag between the gas and the solid phases and S_{other} is a term considered to account for other sources not shown explicitly in Eq. (2).

For gas-solid flows the interphase momentum exchange coefficient K_{pq} can be written in the following general form:

$$K_{pq} = \frac{\alpha_p \rho_p f}{t_p} \tag{3}$$

where α_p and ρ_p are, respectively, the volume fraction and the density of the particle, and t_p is the "particulate relaxation time" defined as:

$$t_p = \frac{\rho_p d_p^2}{18 \mu_q} \tag{4}$$

where μ_q is the viscosity of the gas and d_p is the mean diameter of the particle.

The term f in Eq. (3) includes a drag function (C_D), which differs among different drag models. In the present work the drag models of Wen and Yu (1966) and Gidaspow et al. (1992) were used. In the drag model by Wen and Yu (1966) the interphase momentum exchange coefficient K_{pq} and the drag function C_D assume the following forms:

$$K_{pq} = \frac{3}{4} C_D \frac{\alpha_p \alpha_q \rho_q \left|\boldsymbol{v}_p - \boldsymbol{v}_q\right|}{d_p} \alpha_q^{-2.65} \tag{5}$$

$$C_D = \frac{24}{\alpha_q Re_p}\left[1 + 0.15\left(\alpha_q Re_p\right)^{0.687}\right] \tag{6}$$

ISSN 2176-5480

The term Re_p in Eq. (6) is the relative Reynolds number, defined by Richardson and Zaki (1954) as:

$$Re_p = \frac{\rho_q d_p |\boldsymbol{v}_p - \boldsymbol{v}_q|}{\mu_q} \tag{7}$$

The drag model by Gidaspow et al. (1992) is a combination of the model by Wen and Yu (1966) and the Ergun equation (Ergun, 1952). In this case, when $\alpha_q > 0.8$ the interphase momentum exchange coefficient K_{pq} and the drag function C_D are calculated by the equations of the model by Wen and Yu (1966), that is, by Eq. (5) and Eq. (6), respectively. On the other hand, when $\alpha_q \leq 0.8$ the interphase momentum coefficient K_{pq} assume the following form:

$$K_{pq} = 150\frac{\alpha_p(1-\alpha_q)\mu_q}{\alpha_q d_p^2} + 1.75\frac{\rho_q \alpha_p |\boldsymbol{v}_p - \boldsymbol{v}_q|}{d_p} \tag{8}$$

The model by Gidaspow et al. (1992) is recommended for dense fluidized beds (ANSYS, 2011).

The coupling between the pressure and the velocity fields is accomplished by a Phase-Coupled SIMPLE algorithm (Vasquez and Ivanov, 2000), which is an extension of the SIMPLE algorithm (Patankar, 1980) to multiphase flows.

2.2 Solid phase

The motion of the particles is tracked by the Newtonian Equations of motion, as follows:

$$m\frac{d\boldsymbol{v}}{dt} = \boldsymbol{F}_{drag} + \boldsymbol{F}_{pressure} + \boldsymbol{F}_{gravitation} + \boldsymbol{F}_{other} \tag{9}$$

$$\frac{dx}{dt} = \boldsymbol{v} \tag{10}$$

In Equations (9) and (10) the terms $\boldsymbol{v}_p$, x and m are the velocity, the position and the mass of the particle, respectively. $\boldsymbol{F}_{drag}$, $\boldsymbol{F}_{pressure}$ and $\boldsymbol{F}_{gravitation}$ are the forces acting on the particle due to drag, pressure gradient and gravitation, respectively. The term $\boldsymbol{F}_{other}$ is related to other types of forces not showed explicitly in Eq. (9) and it is in this term that the forces due to the particle interactions calculated by the DEM are included. In the present work, the DEM collision model used for the particle contact force calculation is the Linear Spring/Dashpot (LSD) Model based on the work by Cundall and Strack (1979), which is the only DEM model currently implemented in the software ANSYS FLUENT. In this implementation the rotational motion of the particles is not considered.

For the Linear Spring/Dashpot Model a unit vector ($\boldsymbol{e}_{12}$) is defined pointing from the center of the particle 1 to the center of the particle 2 as follows:

$$\boldsymbol{e}_{12} = \frac{x_2 - x_1}{\|x_2 - x_1\|} \tag{11}$$

where x_1 and x_2 represent the positions of the particles 1 and 2, respectively. The overlap (δ) at the contact point between two colliding particles is:

$$\delta = \|x_2 - x_1\| - (r_1 + r_2) \tag{12}$$

where r_1 and r_2 are the radii of the particles 1 and 2, respectively.

The so-called reduced mass m_{12} and the collision time between two particles t_{coll} are defined as:

$$m_{12} = \frac{m_1 m_2}{m_1 + m_2} \tag{13}$$

$$t_{coll} = \sqrt{\pi^2 + (\ln \eta)^2} \cdot \sqrt{\frac{m_{12}}{K}} \tag{14}$$

where m_1 and m_2 are the masses of the particles 1 and 2, respectively, η is the restitution coefficient and K is the spring constant.

ISSN 2176-5480

The damping coefficient γ and the relative velocity $\boldsymbol{v}_{12}$ between particles 1 and 2 are calculated by:

$$\gamma = -2\frac{m_{12}\ln\eta}{t_{coll}} \tag{15}$$

$$\boldsymbol{v}_{12} = \boldsymbol{v}_2 - \boldsymbol{v}_1 \tag{16}$$

where $\boldsymbol{v}_1$ and $\boldsymbol{v}_2$ are the velocities of the particles 1 and 2, respectively.

After Eqs. (11) through (16) have been evaluated, the normal force applied on the particle 1 is calculated by:

$$\boldsymbol{F}_1 = \left(K\delta + \gamma(\boldsymbol{v}_{12}.\boldsymbol{e}_{12})\right)\boldsymbol{e}_{12} \tag{17}$$

The force applied on the particle 2 is then calculated by considering Newton's third law:

$$\boldsymbol{F}_2 = -\boldsymbol{F}_1 \tag{18}$$

The force due to friction between the particles ($\boldsymbol{F}_f$) is based in the equation for Coulomb friction:

$$\boldsymbol{F}_f = \mu\boldsymbol{F}_n \tag{19}$$

where $\boldsymbol{F}_n$ is the force acting in the direction normal to the surface of the particle and μ is the friction coefficient.

In the present work it was tested the approach of using unrealistic low values for the particle spring constant in the LSD model, since this allows a higher DEM time step to be used and, consequently, a reduction in the total simulation time (Tsuji et al., 1993). This is possible because the DEM time step is a fraction of the collision time, and this collision time increases when the value of the spring constant decreases (See Eq. 14).

According to Hilton and Cleary (2012), real systems usually involve a high number of actual particles and sometimes it is useful to use in CFD-DEM simulations a representative particle model, in which one "coarse scale" DEM particle represents a collection of actual "fine scale" particles, as can be seen in Fig. 1. In the present work a similar approach is used so that a "particle parcel" represents a collection of smaller real particles in order to decrease the number of particles tracked and, consequently, the time required for the simulation.

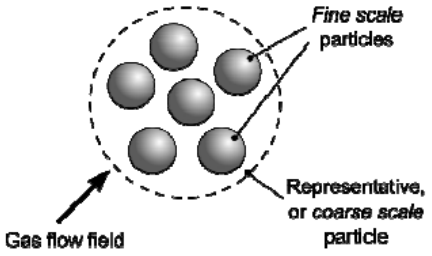

Figure 1. A coarse scale particle representing a collection of fine scale particles (Hilton and Cleary, 2012)

3. MATERIALS AND METHODS

In order to validate the application of the CFD-DEM coupling to alumina fluidization it were employed the experimental data obtained by Lourenço (2012). The alumina used is classified in the Geldart group B (Geldart, 1973), produced at Alunorte – Alumina do Norte do Brasil S.A and used at Albras – Alumínio Brasileiro S.A for the production of primary aluminum. Some characteristics of this alumina are showed in Tab. 1:

Table 1. Some characteristics of the alumina

PROPERTIES	VALUE	DETERMINATION
Density ρ_s (kg/m^3)	3387[(1)]	Picnometry
Mean diameter d_p (μm)	84.06	Sieving
Sphericity (-)	0.679	Image analysis

Source: Adapted from Lourenço (2012).
[(1)]Vasconcelos (2011).

ISSN 2176-5480

The mean diameter showed in Tab. 1 is related to the size distribution of the alumina particles showed in Fig. 2:

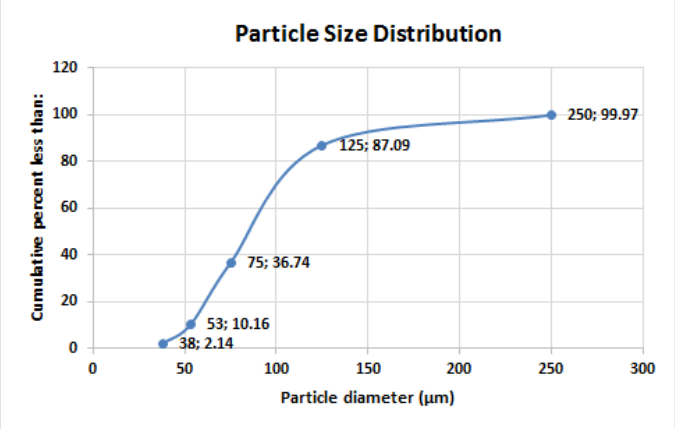

Figure 2. Particle size distribution of the alumina (adapted from Lourenço, 2012)

The fluidization device used to fluidize the alumina bed can be roughly divided into three sections, namely, the plenum chamber, the fluidization chamber and a filter. A simplified representation of this device can be seen in Fig. 3 (dimensions in meter):

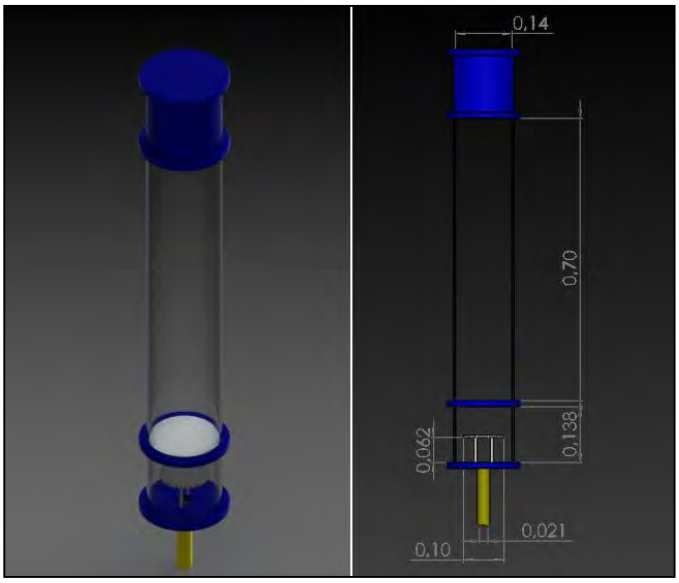

Figure 3. Simplified representation of the fluidization device (adapted from Lourenço, 2012).

The bed operational conditions analyzed in the simulations are summarized in Tab. 2:

Table 2. Operational conditions considered in the CFD-DEM simulations

Material	Alumina
Initial height of the bed (H)	0.1 m
Bed diameter (D)	0.14 m
Aspect ratio (H/D)	0.71
Initial voidage	0.63
Fluidizing gas	Air
Velocities of the fluidizing gas	[0 – 0.125 m/s]

ISSN 2176-5480

The computational domain considered in the simulations is the internal volume of the fluidization chamber showed in Fig. 3. This computational domain was used for the generation of two different meshes, as can be seen in Fig. 4:

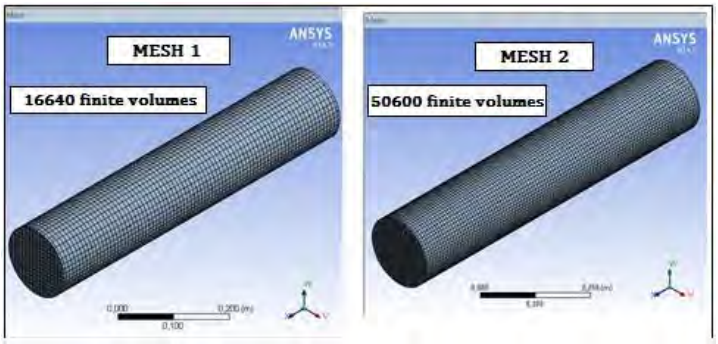

Figure 4. Finite volume meshes used in the simulations

Both of the meshes shown in Fig. 4 are composed by hexahedral elements aligned with the flow direction in order to help in the problem convergence. The main difference between them is that the mesh 1 has 16640 finite volumes, while the mesh 2 has 50600 finite volumes.

In the simulations it were used three different settings for the CFD-DEM model, called here as models A1, A2 and A3. The main characteristics of those models can be seen in Tab. 3 and Tab. 4:

Table 3. The main characteristics of the model A1

MODEL A1			
Diameter of the particle parcel	2.16 mm	**DEM time step**	$2x10^{-04}$ s
Mean diameter of the real particle	84.06 μm	**CFD time step**	$1x10^{-03}$ s
Shape of the virtual particle	Sphere	**Drag model**	Wen and Yu (1966)
Number of particle parcels	100000	**CFD mesh**	Mesh 1
Particle size distribution	Not included	**Fluid flow regime**	Laminar
Coefficient of restitution (particle-particle and particle-wall)	0.9	**Pressure-velocity coupling scheme**	Phase Coupled SIMPLE
Sticking friction coefficient (particle-particle and particle-wall)	0.3	**Boundary condition at the inlet**	Velocity
Gliding friction coefficient (particle-particle and particle-wall)	0.12	**Boundary condition at the outlet**	Pressure
Spring constant K	100 N/m	**Boundary condition at the walls**	Adiabatic, no-slip

Table 4. The main characteristics of the models A2 and A3

MODEL A2	
Drag model	Gidaspow et al.(1992)
Particle size distribution	Yes, included.
Other characteristics	Equal to model A1
MODEL A3	
Diameter of the particle parcel	1.48 mm
Number of particle parcels	300000
Particle size distribution	Yes, included.
Spring constant K	300 N/m
DEM time step	$1.45x10^{-05}$s
CFD time step	$5x10^{-04}$ s
Drag model	Gidaspow et al.(1992)
CFD mesh	Mesh 2
Other characteristics	Equal to model A1

ISSN 2176-5480

4. RESULTS AND DISCUSSION

Firstly, the CFD-DEM simulations were carried out with model A1 for the range of velocities of the fluidizing gas shown in Tab. 2. Figure 5 shows some particle flow patterns of the bed behavior during the 6 initial seconds of fluidization with the air flowing with velocity V_{gas} = 0.075 m/s.

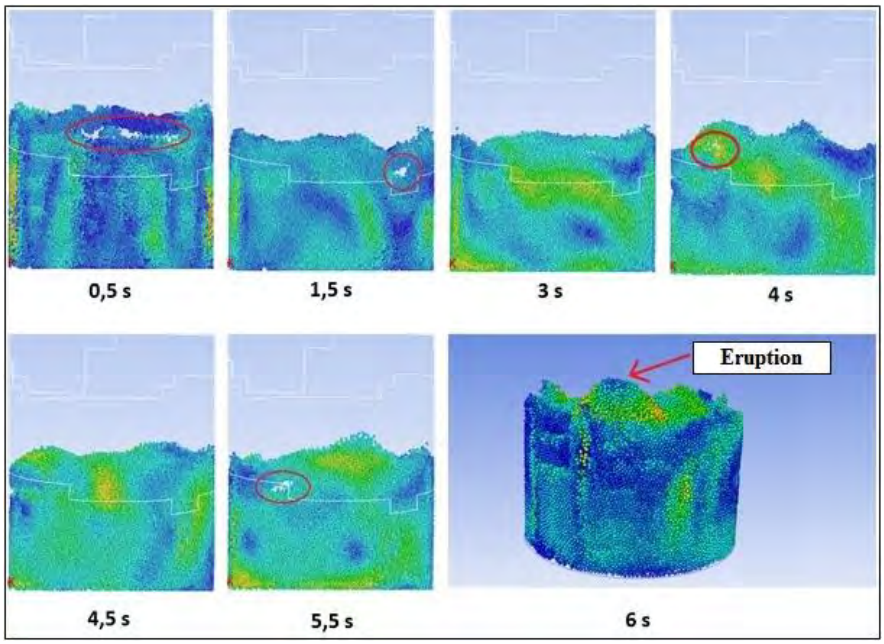

Figure 5. Particle flow patterns colored by velocity magnitude, where the blue color indicates the lower velocities and the green and red colors indicate higher velocities.

Figure 5 shows the bed height at 0.5s higher because an initial blow of air was used in order to generate a bed in which the particles have random initial positions. Some bubbles and the eruption phenomenon are also indicated in Fig. 5, typically the behavior of particles of the Geldart group B.

In each simulation analyzed in this paper, the instantaneous area weighted average value of the fluid pressure was monitored during 6 seconds at the inlet of the domain (the bottom of the bed). After that, the time average value of that pressure signal was taken. This procedure was repeated for different values of the fluid velocity and the corresponding values of the time averaged pressure were used for the needed comparisons (e.g. Fig.6 and Fig. 7, etc.).

In order to analyze the results obtained with the CFD-DEM simulations in which the model A1 was used, those simulated results were compared with the experimental data obtained by Lourenço (2012) (See Fig. 6 and Tab 5):

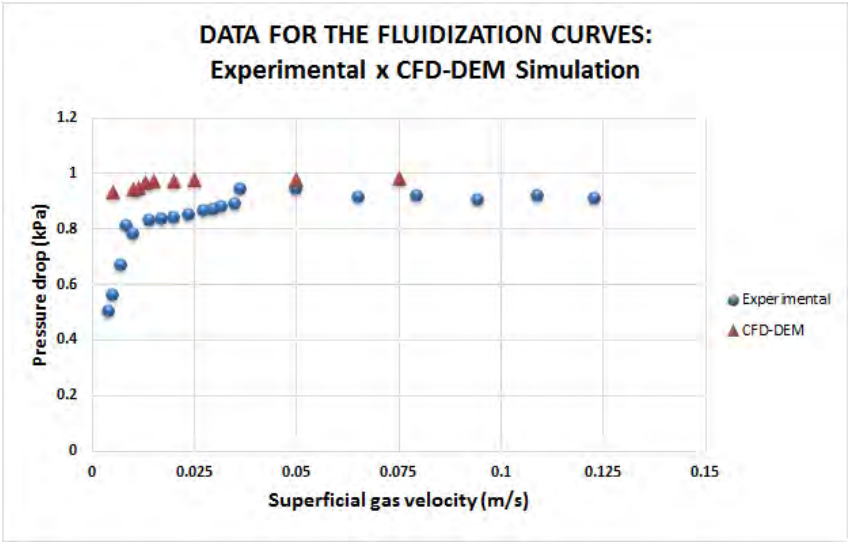

Figure 6. Data for fluidization curves obtained by experiments and by simulations using model A1

ISSN 2176-5480

Table 5. Pressure drop data obtained by experiments and by simulations with model A1

Velocity (m/s)	ΔP_{exp} (kPa)	ΔP_{sim} (kPa)	Error (%)
0.0050	0.5600	0.9354	40.13
0.0100	0.7800	0.9412	17.12
0.0115	0.8000	0.9481	15.62
0.0129	0.8220	0.9680	15.08
0.0150	0.8259	0.9720	15.03
0.0200	0.8384	0.9742	13.93
0.0250	0.8571	0.9763	12.21
0.0500	0.9440	0.9765	3.32
0.0750	0.9301	0.9805	5.14

As can be seen in Fig. 6 and Tab. 5, it was not possible to obtain good agreement between experimental and simulated data for the pressure drop values in the region of the fixed bed when using model A1 in the simulations. For the gas velocity $V_{gas} = 0.005$ m/s the approximate error was of about 40% which is clearly unacceptable. However, if one plots only the simulated data against the superficial gas velocity, the curve obtained has the shape of a typical fluidization curve and an estimate of the minimum fluidization velocity can be obtained, as shown in Fig. 7:

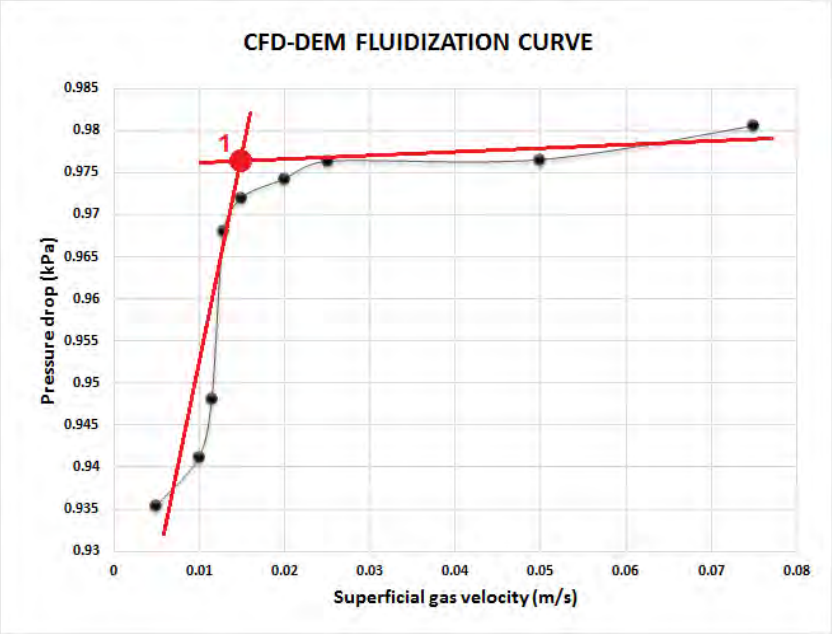

Figure 7. Fluidization curve obtained by simulations using model A1

In Figure 7, the minimum fluidization velocity estimated by using the simulation data is the one related to the point 1, which is the point where the line representing the fixed bed region intercepts the line representing the fluidized bed region. For the point 1, the simulated minimum fluidization velocity is $V_{mf} = 0.015$ m/s, which is in good agreement with the experimental value of $V_{mf} = 0.0129$ m/s. The pressure drop value for the minimum fluidization condition was predicted by the CFD-DEM simulation as $\Delta P_{sim} = 0.977$ kPa, which is also in good agreement with the experimental value reported as being $\Delta P_{exp} = 0.95$ kPa (This experimental value was also determined by the interception between the fixed bed line and the fluidized bed line in the experimental fluidization curve by Lourenço (2012)).

Even being possible to predict the minimum fluidization behavior of the alumina bed with the model A1, as described above, it was considered that this kind of approach could be somewhat uncertain, since with model A1 the predictions for the pressure drop values in the region of fixed bed were very different from the experimental values. This led to the search for the adjustment of the CFD-DEM model so that it could be capable of predicting the alumina bed's behavior in the whole range of gas velocities analised in this work.

ISSN 2176-5480

The suspicions for the limitations of the model A1 to predict the alumina fixed bed's behaviour were not limited to the fact that an unrealistic lower spring constant was used for the DEM model, but also to the fact that the CFD and DEM time steps were not small enough, the drag model of Wen and Yu (1966) is not so appropriate for dense systems, the particulate system was being considered to be a system of uniformely sized particles and that the particle and CFD mesh resolutions (number and size) should be improved. The choice of the majority of the parameters described before was initially set in the model A1 in such a way that the total runtime of the simulations could be reduced, but this can have prejudiced the predictions of the fixed bed regime, what indicates that care must be taken when trying to reduce the total simulation time

In order to improve the capabilities of the CFD-DEM model, the model A1 was modified and new simulations were carried out for the gas velocity of $V_{gas} = 0.005$ m/s, which is a gas velocity in which the real alumina bed is in the fixed bed regime. The first modifications done to the model A1 were the inclusion of the particle size distribution of the particulate system and the drag model of Gidaspow et al. (1992), which is more suitable for dense beds. This new model was called model A2, as can be seen in Tab. 4. Aditionally, more modifications were done to the model A2 in order to create a new model called model A3, in which the main characteristics were the increase in the spring constant of the DEM model from 100 N/m to 300 N/m, the decrease in the values of the DEM and CFD time steps, the decrease in the size of the particle parcels and the consequent increase in the number of particle parcels in the virtual system.

The main characteristics of the models A1, A2 and A3 were sumarized in Tab. 3 and Tab. 4 and the comparison of the results obtained with those three models for the gas velocity of $V_{gas} = 0.005$ m/s are showed in Fig. 8:

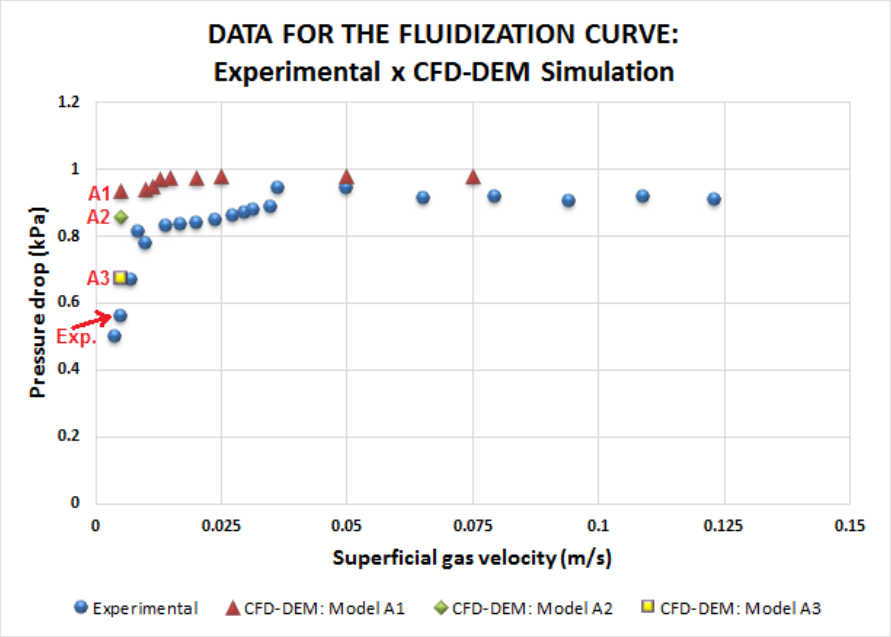

Figure 8. Comparison of results obtained with models A1, A2 and A3 for $V_{gas} = 0.005$ m/s.

Figure 8 indicates the pressure drop values corresponding to the gas velocity of $V_{gas} = 0.005$ m/s obtained with experiments (blue sphere) and with the CFD-DEM models A1, A2 and A3. As can be seen in Fig. 8 the pressure drop predicted by the model A2 is closer to the experimental value (blue sphere) than the one predicted by the model A1. Also the pressure drop predicted by the model A3 is closer to the experimental value (blue sphere) than the one predicted by the models A1 and A2. In Table 6 one can compare the errors related to the comparison with the experimental value of the pressure drop for the gas velocity of $V_{gas} = 0.005$ m/s:

Table 6. Comparison of results obtained with models A1, A2 and A3.

MODEL	Velocity (m/s)	ΔP_{exp} (kPa)	ΔP_{sim} (kPa)	Error (%)
Model A1	0.005	0.56	0.9354	40.13
Model A2	0.005	0.56	0.8550	34.50
Model A3	0.005	0.56	0.6731	16.8

ISSN 2176-5480

5. CONCLUSIONS

Even the results presented in this paper being only partial results from a deeper work still in progress, they allowed to notice the importance of some aspects to be considered when applying the CFD-DEM coupling in fluidization. When trying to reduce the simulation time by means of using high values for the DEM and CFD time steps and unrealistic low values for the spring constant in the context of the Linear Spring/Dashpot model, care must be taken in order to avoid the loss in terms of prediction capacity. However, remembering the complexity of the two-phase flow analyzed here and the assumptions considered, it is believed that the results allowed to check the possibility of using the simple Linear Spring/Dashpot Model to predict the global behavior of alumina fluidized beds, since the model parameters are set correctly.

6. ACKNOWLEDGMENTS

The authors would like to thank CAPES, CNPq, FAPESPA and VALE S.A for the financial support.

7. REFERENCES

ANSYS, Inc., 2011. *ANSYS FLUENT theory guide*. Canosnburg, USA.

Crowe, C. T., 2006. *Multiphase Flow Handbook.* CRC Press, Boca Raton.

Cundall, P. A. and Strack, O. D. L., 1979. "A discrete numerical model for granular assemblies". *Geotechnique,* Vol. 29, p. 47 – 65.

Ergun, S., 1952. "Fluid flow through packed columns". *Chem. Eng. Prog.,* Vol. 48, p. 89 – 94.

Fleissner, F. and Eberhard, P., 2008. "Parallel load-balanced simulation for short-range interaction particle methods with hierarchical particle grouping based on orthogonal recursive bisection". *International Journal for Numerical Methods in Engineering,* Vol. 74, p. 531 – 553.

Fraige, F. Y. and Langston, P. A. 2004. "Integration schemes and damping algorithms in distinct element models". *Advanced Powder Technology,* Vol. 15, p. 227 – 245.

Geldart, D., 1973. "Types of gas fluidization". *Powder Technology,* Vol. 7, p. 285 – 292.

Gidaspow, D., Bezburuah, R. and Ding, J., 1992. "Hydrodynamics of circulating fluidized beds: Kinetic Theory approach". In *Proceedings of the 7th Engineering Foundation Conference on Fluidization.*

Gidaspow, D., 1994. *Multiphase flow and fluidization: Continuum and kinetic theory description.* Academic Press.

Hilton, J. E. and Cleary, P. W., 2012. "Comparison of resolved and coarse grain DEM models for gas flow through particle beds". In *Proceedings of the Ninth International Conference on CFD in the Minerals and Process Industries.* Australia.

Iwai, T., Hong, C. W. and Greil, P., 1999. "Fast particle pair detection algorithms for particle simulations". *International Journal of Modern Physics,* Vol. 10, p. 823 – 838.

Limtrakul, S. et al., 2003. "Discrete particle simulation of solids motion in a gas-solid fluidized bed". *Chemical Engineering Science,* Vol. 58, p. 915 – 921.

Lourenço, R.O., 2012. *Análise experimental e numérica da fluidização para aplicações industriais.* Ph.D. thesis, Universidade Federal do Pará, Brasil.

Malone, K. F. and Xu, B. H., 2008. "Determination of contact parameters for discrete element method simulations of granular systems". *Particuology,* Vol. 6, p. 521 – 528.

Mikami, T., Kamiya, H. and Horio, M., 1998. "Numerical simulation of cohesive powder behavior in a fluidized bed". *Chemical Engineering Science,* Vol. 53, p. 1927 – 1940.

MME (Ministério de Minas e Energia do Brasil)., 2011. National Mining Plan 2030. Brasília.

Niemi, T., 2012. *Particle size distribution in CFD simulation of gas-particle flows*. M.Sc. thesis, Aalto University, Finland.

Patankar, S. V., 1980. *Numerical Heat Transfer and Fluid Flow.* Hemisphere, Washington, DC.

Rhodes, M. J. et al., 2001. "Use of discrete element method simulation in studying fluidization characteristics: Influence of interparticle force". *Chemical Engineering Science,* Vol. 56, p. 69 – 76.

Richardson, J. R. and Zaki, W. N., 1954. "Sedimentation and Fluidization: Part I". *Trans. Inst. Chem. Eng.,* Vol. 32, p. 35 – 53.

Tsuji, Y., Kawaguchi, T. and Tanaka, T., 1993. "Discrete particle simulation of two-dimensional fluidized bed". *Powder Technology,* Vol. 77, p. 79 – 87.

Vasconcelos, P. D. S., 2011. *Transporte pneumático fluidizado: Estudos de casos aplicados à indústria do alumínio primário.* Ph.D. thesis, Universidade Federal do Pará, Brasil.

Vasquez, S. A. and Ivanov, V. A., 2000. "A phase coupled method for solving multiphase problems on unstructured meshes". In *Proceedings of ASME FEDSM'00. ASME 2000 Fluids Engineering Division Summer Meeting. USA.*

Wen, C. Y. and Yu, Y. H., 1966. "Mechanics of fluidization". *Chem. Eng. Progress Symp. Series,* Vol. 62, p. 100-111.

ISSN 2176-5480

Zhu, H. P. et al., 2007. "Discrete particle simulation of particulate systems: Theoretical developments". *Chemical Engineering Science,* Vol. 62, p. 3378 – 3396.
Zhu, H. P. et al., 2008. "Discrete particle simulation of particulate systems: A review of major applications and findings". *Chemical Engineering Science,* Vol. 63, p. 5728 – 5770.

8. RESPONSIBILITY NOTICE

The authors are the only responsible for the printed material included in this paper.